JOURNAL OF SPACECRAFT AND ROCKETS
Vol. 45, No. 5, September–October 2008

Fault-Tolerant Stabilization of a Tethered Satellite System Using Offset Control

Godard,* K. D. Kumar,† and B. Tan‡
Ryerson University, Toronto, Ontario M5B 2K3, Canada

DOI: 10.2514/1.35029

An adaptive fault-tolerant nonlinear control design based on the theory of sliding mode is proposed to control the attitude of a satellite using coordinated movement of the tether attachment points. The system consists of two identical tethers of equal length connecting the downward-deployed auxiliary mass to two distinct points that are symmetrically offset from the satellite mass center. This paper examines cases when tether deployment suddenly stops and tether breakage occurs. The nonlinear analytical model describing the system is used to derive a nominal sliding mode control law and an adaptive fault-tolerant control law in the presence of unknown slow-varying satellite mass distribution and tether rigidity parameters. Several numerical examples are presented to demonstrate the efficacy of the proposed control algorithms. Final results show that the high-amplitude oscillations present in the in-plane motion of the main satellite due to tether severance are effectively damped within a quarter of an orbit. In addition, an abrupt blockage of one of the tether attachment points is simulated, and the control law verifies the possibility of controlling the attitude of the satellite. The numerical results clearly establish the robustness of the proposed adaptive offset control scheme in regulating the satellite dynamics of a two-tether system in the event of breakage of one of the tethers.

Nomenclature

a_j, b_j	=	z and y coordinates or horizontal and vertical offsets of tether attachment points A ($i = 1$) and B ($i = 2$) in the satellite S–$x_0y_0z_0$ coordinate frame, m
$\bar{a}_j, \bar{b}_j$	=	$a_i/L_{\text{ref}}, b_i/L_{\text{ref}}$
C_j	=	$EA/(m_2L_{\text{ref}}\Omega^2)$ ($j = 1, 2$), tethered satellite systems rigidity parameter
EA	=	tether modulus of rigidity, N
f_i	=	ith constraint function, $i = 1, 2$
I_k	=	satellite principal centroidal moments of inertia about the k axis, $k = x, y, z$, kg-m^2
I_r	=	satellite mass distribution parameter; $(I_y - I_z)/I_x$
L	=	distance of the auxiliary mass from the satellite mass center, m
L_j	=	stretched tether lengths, $j = 1, 2$, m
L_{j0}	=	unstretched tether lengths, $j = 1, 2$, m
L_{ref}	=	reference length, $(I_x/m_2)^{1/2}$, m
l, l_j, l_{j0}	=	$L/L_{\text{ref}}, L_j/L_{\text{ref}}, L_{j0}/L_{\text{ref}}$, respectively
M	=	mass of the satellite, kg
m_2	=	mass of the auxiliary body, kg
R	=	orbital radius, m
α	=	satellite pitch angle, deg
β	=	in-plane tether swing angle, deg
ε_j	=	tether strains in the jth tether
θ	=	in-plane angle measured relative to a specified reference line, deg
Λ_i	=	Lagrange multiplier for the ith constraint
μ	=	Earth's gravitational constant, m^3/s^2
μ_1, υ	=	derivative and proportional control gains
Ω	=	angular velocity, $(\mu/R^3)^{1/2}$, rad/s

Received 7 October 2007; revision received 7 March 2008; accepted for publication 1 April 2008.

*Graduate Student, Department of Aerospace Engineering, 350 Victoria Street; ggodard@ryerson.ca.

†Associate Professor and Canada Research Chair in Space Systems, Department of Aerospace Engineering, 350 Victoria Street; krishnadevkumar@yahoo.com. Member AIAA (Corresponding Author).

‡Assistant Professor, Department of Aerospace Engineering, 350 Victoria Street; tanbo@ryerson.ca.

I. Introduction

THE advent of tethered satellite systems (TSS) [1] marks the beginning of a new era in space research. Several interesting space applications of tethers have been proposed and several missions have been flown [2]; some missions were successful and others were unsuccessful. The major successful missions include the Canadian Space Agency's Observation of Electric-Field Distributions on the Ionospheric Plasma—A Unique Strategy (OEDIPUS) missions: OEDIPUS-A in 1989 and OEDIPUS-C in 1995 [3,4], NASA's Small Expendable Deployer System (SEDS) missions: SEDS-1 in 1993 and SEDS-2 in 1994 [5], NASA's Plasma Motor Generator (PMG) experiment in 1993 [6], and the U.S. Naval Research Laboratory's tether physics and survivability (TiPS) in 1996 [7]. Some of the unsuccessful missions were the NASA and Italian Space Agency's (ASI) TSS-1 in 1992 [8] and NASA's Advanced Tether Experiment (ATEx) in 1998 [9]. Some of the major causes of failure of these missions were found to be associated with tether deployment and tether breakage. Researchers have tried to solve these problems using a high-performance tether deployment system and multistrand tethers; however, the problems of tether deployment and breakage still exist. The scope of this paper is to emphasize the challenges associated with the attitude stabilization of a two-tether system when tether deployment suddenly stops and tether breakage occurs. We address the attitude control of a spacecraft using two identical tethers of equal length connecting a downward-deployed auxiliary mass. The tethers are connected to two distinct points symmetrically offset from the spacecraft's mass center. The objective is to control the attitude of the spacecraft through regulated motion of the tether attachment point.

The dynamics and control aspects of the TSS have received considerable attention by several researchers in the last two decades. An excellent review of the dynamics and control aspects of TSS was done by Kumar [10]. Some of the contemporary investigations focused on the deployment of a subsatellite mass through two or more tethers. A comprehensive review of the earlier work on tethered satellites was treated by Misra and Modi [11,12], focusing primarily on single-tether two-body systems. Misra and Diamond [13] proposed a TSS model comprised of a subsatellite and a main satellite body connected by two extensible, but massless, tethers.

They considered the TSS motion in a circular orbit along with tether in-plane motion, out-of-plane motion, and longitudinal oscillations. Their observation of a two-tether system indicated a superior rotational behavior when compared with a single-tether system, but was found to have adverse tether longitudinal oscillations. A hybrid control to regulate tether lengths by using a simple bitethered pendulum mass was proposed by Kumar and Kumar [14]. In their analysis, high satellite pointing precision was achieved with significantly shorter tether lengths.

In the presence of an offset between the tether attachment point and the mass center of the end satellite, termed the tether offset, the satellite experiences additional moments, and its attitude motion becomes coupled to that of the tether librational motion [15]. The choice of tether offset has a significant effect on the system transient response [16]. A study on the dynamics and control aspects of a space platform in the presence of tether offset was undertaken by Fan and Bainum [17]. For the requirement of disturbance rejection, the motion of the tether attachment point along the roll and pitch axes can produce the pitch and roll control moments, respectively [18]. A precision pointing offset control algorithm for the TSS was developed using an linear quadratic regulator feedback law and a Kalman filter to regulate the subsatellite motion [19]. In [20], the tether offset control scheme involving time-dependent motion of the tether attachment point was found to be successful in damping the momentum of a main satellite having initial momentum. The effectiveness of this scheme was validated by Modi et al. [21] through a ground-based experiment as well as a numerical simulation. An orbiting-platform-supported tethered subsatellite system was analyzed by Modi et al. [22], who studied the effectiveness of an offset control strategy numerically and substantiated its validity through a ground-based experiment. For large disturbances, the offset control was found to be effective both during stationkeeping as well as retrieval maneuver. In a subsequent study [23], three different control strategies (thruster control, tension control, and offset control, as well as their combinations) were compared, and it was found that the thruster-offset hybrid controller is the most effective in damping disturbances.

Controllers for the TSS attitude and vibrational motion were designed by Pradhan et al. [24] using a feedback linearization technique and a robust linear-quadratic-Gaussian/loop transfer recovery, respectively. Their analysis indicated that the tether offset scheme was found to be effective in simultaneous control of the platform and tether pitch motion for a shorter tether. A controller design using a graph theoretic approach was considered by Modi et al. [25]. For a smaller end satellite such as SEDS's payload [26], a long rigid appendix at the tether attachment point is effective at stabilizing the satellite's attitude. In [27], rigid booms and fins were applied for drag stabilization, a tether offset control was used for the payload attitude control, and a thruster was used for the tether librational control. The application of only tether offset variations for the orientation control of the main satellite with a single tether was studied by Modi et al. [28] using a Lyapunov control strategy. In [29], a simple open-loop tether offset control law for attitude maneuver of dual satellite platforms connected by a relatively short tether was proposed. However, the system has the limitation of controlling yaw excitation in the case of roll maneuver. Pines et al. [30] presented an analysis of the dynamics and control of the pitch and roll motion during retrieval of a TSS, consisting of the Space Shuttle Orbiter and the tethered satellite. Phase-plane switch logic and visual observation of line-of-sight angle were used to generate rules for orbiter pilots. An adaptive control technique on an orbiting single TSS was presented by Walls and Greene [31]. Performance was rated based on the effectiveness of the controller in performing station-keeping maneuvers. Nohmi et al. [32] proposed a cooperative control approach to employ a momentum-assisted tether-extension strategy for a tethered space robot deployed from a spacecraft. The translation to the destination point was controlled using the manipulator arm on the spacecraft, and the angular momentum that changes with tether tension variation was controlled using the tether attachment point on the subsatellite. Gravity force and centrifugal force were not considered to influence tether extension. The tether attachment-point control is designed based on a proportional–derivative control scheme and is used as a disturbance during casting for the trajectory adjustment control. Williams et al. [33] considered the feasibility of using the tether attachment point on the main satellite to absorb in- and out-of-plane traveling waves along the tether. Electromagnetic Lorentz forces are used as a control actuator for controlling the librational dynamics of the TSS. A nonlinear hybrid control law is derived using Lyapunov's second method that combines tether tension control with current control. The control is asymptotically stable in a low-order model of the system dynamics, but leads to instability in the lateral modes when tether flexibility and elasticity is accounted for. The instability is mitigated by applying a wave-absorption control scheme, which employs movement of the tether attachment point.

Although the offset control scheme has been used in different tethered systems, none of the preceding literature account for unexpected severance of the tether, which is a major problem associated with multiple tethered satellite systems. Trivailo et al. [34] investigated the initiation and process of two unscheduled events, tether severance and interference between tether and other hardware, using a high-speed computer simulation incorporating a nonlinear lumped-mass model. Williams et al. [35] considered the deployment, retrieval, and rendezvous scenarios of a platform and subsatellite connected via two tethers using both linear and nonlinear control techniques implemented via tension control. The flexible-tether model developed is used to simulate the event of tether severance. Some of the potential problems that can occur due to tether severance include the following [35]:

1) The loss of tension at the severance point causes the tether to accelerate away from the platform.

2) The tether rotates around the attachment at the subsatellite.

3) The tether becomes entangled in itself and does not rotate around the attachment at the subsatellite.

A severed tether can also recoil and wrap around the platform [36]. Although tether severance is numerically simulated in [34,35], the issue of attitude control using the remaining tether has not received its due attention in the literature.

With a view to overcome this limitation, this paper considers the attitude stabilization of a two-tether system in the event of breakage of one of the tethers, using nonlinear control techniques implemented via offset control. The main contributions of this study relative to other works are as follows.

1) A nonlinear control technique based on sliding mode theory is proposed to control the attitude of a two-tether subsatellite system using coordinated movement of the tether attachment points. In comparison with the aforementioned studies [14–36] associated with the dynamics and control of TSS, this study considers the case when tether deployment suddenly stops and one of the tethers is severed.

2) A fault-tolerant adaptive sliding mode control scheme is proposed to stabilize the attitude of the main satellite in the event of breakage of one of the tethers. Furthermore, a likely scenario in which one of the two tether attachment points suddenly stops moving is incorporated to test the effectiveness of the proposed nonlinear control laws.

In this study, we do not account for collision dynamics of the tether with itself or the second tether, and hence the consequence of tether entanglement is not assessed. Similarly for the case of tether severance, tether recoil and wrapping of the remaining tether around the main satellite is not considered. The paper is organized as follows. Section II introduces the mathematical model of the system and the offset control strategy. Nominal sliding mode control and the fault-tolerant adaptive control laws are formulated in Sec. III. For a detailed assessment of the system performance under the proposed control strategies, the results of the computer simulations are presented in Sec. IV. In Sec. V, we conclude this paper with some discussions on future work.

II. TSS Model and Equations of Motion

The investigation is initiated by formulating the equations of motion of the proposed TSS moving in a circular orbit. The proposed

system model assumes a downward deployment of a small auxiliary mass from the satellite through a two-tether system (Fig. 1). Two identical tethers are attached to the satellite at two distinct points symmetrically offset from its mass center and below the satellite's principal z axis. The other ends of the two tethers are connected to an auxiliary mass. To facilitate analytical treatment of the problem, only the case involving in-plane system motion is investigated.

The coordinate frame S–$x_0y_0z_0$ passing through the system center of mass represents the orbital reference frame. The right-hand triad is formed with the x_0 axis taken normal to the orbital plane, the y_0 axis taken along the local vertical, and the z_0 axis pointing along the local horizontal. The measured spacecraft orientation is a rotation α of the local frame about the x_0 axis. Hence, the angle α defines the librational pitching angle with respect to the local vertical. The S–xyz coordinate frame is used to represent the relative motion of the spacecraft with respect to the local orbital frame. For the variable length $\mathbf{L}$ joining the satellite mass center S and tether junction E, the angle β denotes rotation about the axis normal to the orbital plane and is referred to as the in-plane swing angle.

The satellite pitch angle α, the distance between the satellite mass center and the auxiliary mass ($\mathbf{L}$), its associated in-plane swing angle β, and the two tether strains ε_1 and ε_2 constitute the chosen set of generalized coordinates that describe the motion of the system. The preceding generalized variables are not independent and they are related through dimensionless constraints as follows:

$$\begin{aligned} f_1 &= l_1 - (\bar{a}_1^2 + \bar{b}_1^2 + l^2 - 2l\bar{h}_1)^{\frac{1}{2}} = 0, \\ f_2 &= l_2 - (\bar{a}_2^2 + \bar{b}_2^2 + l^2 + 2l\bar{h}_2)^{\frac{1}{2}} = 0 \end{aligned} \tag{1}$$

The derivations of $\bar{h}_1$ and $\bar{h}_2$ and other dynamic relations and their conversion to dimensionless form are provided in the Appendix. The major assumptions employed in the derivation of the mathematical model are as follows:

1) The main spacecraft M is considered to have greater mass when compared with the tether and the subsatellite m_2, and hence the center of mass of the system is assumed to coincide with the center of mass of the spacecraft.

2) The tether is assumed to be made of light material such as Kevlar, and therefore it is considered to have negligible mass. The damping effects and transverse vibrations of the tethers are ignored. Because of the relatively short tether lengths considered in this study, it is assumed that the tether dynamics do not affect the orbital dynamics.

3) The only external force acting on the system is the Newtonian gravity force.

Application of the Lagrange procedure results in the following nonlinear, nonautonomous, coupled equations of motion governing the system dynamics.

Satellite pitch α:

$$\begin{aligned} &\alpha'' - 1.5I_r \sin(2\alpha) - \frac{\lambda_1}{l_1} l[\bar{a}_1 \cos(\alpha-\beta) - \bar{b}_1 \sin(\alpha-\beta)] \\ &\quad + \frac{\lambda_2}{l_2} l[\bar{a}_2 \cos(\alpha-\beta) + \bar{b}_2 \sin(\alpha-\beta)] = 0 \end{aligned} \tag{2}$$

$\mathbf{L}$ in-plane swing β:

$$\begin{aligned} &\beta'' + 1.5\sin(2\beta) + 2(1+\beta')\left(\frac{l'}{l}\right) \\ &\quad + \frac{\lambda_1}{l_1}(1/l)[\bar{a}_1 \cos(\alpha-\beta) + \bar{b}_1 \sin(\alpha-\beta)] \\ &\quad - \frac{\lambda_2}{l_2}(1/l)[\bar{a}_2 \cos(\alpha-\beta) + \bar{b}_2 \sin(\alpha-\beta)] = 0 \end{aligned} \tag{3}$$

$\mathbf{L}$ dimensionless length l:

$$\begin{aligned} &l'' + [(1 - 3\cos^2\beta) - (1+\beta')^2]l \\ &\quad + \frac{\lambda_1}{l_1}[l - \bar{a}_1 \sin(\alpha-\beta) - \bar{b}_1 \cos(\alpha-\beta)] \\ &\quad + \frac{\lambda_2}{l_2}[l + \bar{a}_2 \sin(\alpha-\beta) - \bar{b}_2 \cos(\alpha-\beta)] = 0 \end{aligned} \tag{4}$$

Tether strains ε_1 and ε_2:

$$\lambda_1 = C_1\varepsilon_1 U(\varepsilon_1), \qquad \lambda_2 = C_2\varepsilon_2 U(\varepsilon_2) \tag{5}$$

From Eqs. (2–5), it is clearly evident that offset positions $\bar{a}_1$ and $\bar{a}_2$ are difficult to extract from the coupled equations to design a control law. On the other hand, choosing the two offset velocities $\bar{a}_1'$ and $\bar{a}_2'$ as control inputs and integrating them to obtain offset positions simplifies the control design procedure. Therefore, the modified form of the pitch equation of motion explicitly showing the control inputs is as follows:

$$\alpha''' = I_r f_0(x) + C_1 f_1(x) + C_2 f_2(x) + C_1 g_1(x)\bar{a}_1' + C_2 g_2(x)\bar{a}_2' \tag{6}$$

As can be expected, the complete set of equations is extremely lengthy and hence is not presented here, for brevity. The complete forms of $f_i(x)$ and $g_i(x)$ ($i = 0, 1, 2$) are provided in the Appendix.

III. Design of Control Laws

In this section, we present the theoretical basis for incorporating TSS attitude control using coordinated motion of tether offsets into the nonlinear control framework. First, the methods and analysis tools of sliding mode nonlinear control are developed that are robust to nonlinear model errors. The formulation of the nominal sliding mode controller is then improved using adaptive approximation in the presence of nonlinear model uncertainty. The desired attitude of the spacecraft is ensured through regulated motion of the tether attachment points $\bar{a}_1$ and $\bar{a}_2$.

A. Nominal Sliding Mode Control

Sliding mode control is a robust nonlinear feedback control methodology that belongs to a kind of variable-structure control system in which the structure between switching surfaces is changed to achieve desired performance. Sliding mode control is insensitive to external disturbances [37] and therefore one can consider it to implement the offset control scheme for TSS. The group of state variables used to construct the sliding surface are α, α', and α''. The sliding surface S is defined as

$$S = \alpha'' + p_2\alpha' + p_1\alpha \tag{7}$$

where p_1 and p_2 are positive constants. The basic idea is to alter the system dynamics along the sliding surface such that the trajectory of the system is steered onto the sliding manifold described by $S = 0$.

Next, we derive the control laws based on the Lyapunov stability theorem. The control law that forces the motion of the states to be along the sliding manifold $S = 0$ can be derived by choosing the Lyapunov energy function defined as follows:

$$V = \tfrac{1}{2}S^2 \tag{8}$$

Differentiating V, we get

$$V' = SS' = S(\alpha''' + p_2\alpha'' + p_1\alpha') \tag{9}$$

Substituting Eq. (6) into Eq. (9), we get

$$\begin{aligned} V' = S[&I_r f_0(x) + C_1 f_1(x) + C_2 f_2(x) + C_1 g_1(x)\bar{a}_1' \\ &+ C_2 g_2(x)\bar{a}_2' + p_2\alpha'' + p_1\alpha'] \end{aligned} \tag{10}$$

Sliding mode control design finds the control law such that SS' is always negative-definite. Let

$$I_r f_0(x) + C_1 f_1(x) + C_2 f_2(x) + p_2\alpha'' + p_1\alpha' + C_1 g_1(x)\bar{a}_1' + C_2 g_2(x)\bar{a}_2' = -\eta\,\mathrm{sat}(S) - kS \tag{11}$$

where η and k are positive constants. The saturation function $\mathrm{sat}(x)$ is used to suppress the control chatter [38]. Alternative switching functions might be used. This choice has no effect on the closed-loop trajectories, except when sliding along the sliding surface S, in which case details of the deadband will strongly influence the high-frequency chatter in the control input [39]. Substituting Eq. (11) into Eq. (10), V' becomes negative-definite. Hence, the system is stable and its trajectory will approach the sliding plane while converging toward the origin.

$$V' = -\eta|S| - kS^2 \le 0 \tag{12}$$

Rearranging the terms in Eq. (11), the control laws can be obtained as

$$\bar{a}_1' = \frac{D_1}{D_1^2 + D_2^2} D_3, \qquad \bar{a}_2' = \frac{D_2}{D_1^2 + D_2^2} D_3 \tag{13}$$

where

$$\begin{aligned} D_1 &= C_1 g_1(x), \\ D_2 &= C_2 g_2(x), \\ D_3 &= -\eta\,\mathrm{sgn}(S) - kS - I_r f_0(x) - C_1 f_1(x) - C_2 f_2(x) \\ &\quad - p_2\alpha'' - p_1\alpha' \end{aligned} \tag{14}$$

For the existence of the control inputs described by Eq. (13), $D_1^2 + D_2^2$ must be nonzero in the region of interest. After carrying out some simplifications, the region $\Omega_S(\Omega_{S_1} \cap \Omega_{S_2})$ of singularity in which $D_1^2 + D_2^2 = 0$ is given by

$$\begin{aligned} \Omega_{S_j} &= \left\{ D_j^2 = C_j^2 \left\{ \frac{1}{\bar{a}_j}\cos(\alpha - \beta) + \frac{\bar{b}_j}{\bar{a}_j}[1 - \sin(\alpha - \beta)] \right\}^2 = 0 \right\} \\ &= \left\{ \left[\frac{1}{\bar{a}_j}\cos(\alpha - \beta) + \frac{\bar{b}_j}{\bar{a}_j}[1 - \sin(\alpha - \beta)] \right] = 0 \right\} \\ &= \left\{ \alpha - \beta = (4n + 1)\frac{\pi}{2} \right\} \end{aligned} \tag{15}$$

where $j = 1, 2$, and $n \in J$ is a set of integers. The control law is well defined as long as the trajectory of the closed-loop system does not enter the region Ω_s. The control inputs $\bar{a}_1$ and $\bar{a}_2$ are obtained by numerically integrating the expressions in Eq. (13) and are then provided to Eq. (2) to complete the closed-loop dynamics of the system.

B. Adaptive Sliding Mode Control

In TSS, parameter uncertainties can pose numerous problems in the control tasks, causing inaccuracy and instability in the control system. Adaptive control deals with situations in which some of the parameters are unknown or slowly time-varying. The basic idea is to estimate these unknown parameters online and then use the estimated parameters in place of the unknown parameters in the feedback control law. Two different types of adaptive control for the TSS are considered in this section.

1) In case I, we use the exact parameter representation I_r, C_1, and C_2. Adaptive control law is developed based on the nominal nonlinear control law designed in Sec. III.A. Although the true values of C_1 and C_2 are equal, we evaluate the controller when their estimated values could differ.

2) In case II, we consider modified system parameters, represented as $\eta_1 = I_r/C$ and $\eta_2 = 1/C$, where $C = C_1 = C_2$.

The tether rigidity parameters are denoted separately with subscripts 1 and 2, to induce tether failure into the model. For example, to consider the failure of tether 2, we set $C_2 = 0$ in the plant. In both cases, the control laws are designed to be fault-tolerant; that is, information regarding the failure of tether 2 is not passed to the control laws.

1. Fault-Tolerant Adaptive Control (Case I)

In this case, I_r, C_1, and C_2 are unknown constant parameters. The parameter estimation errors are given by

$$\tilde{I}_r = \hat{I}_r - I_r, \qquad \tilde{C}_1 = \hat{C}_1 - C_1, \qquad \tilde{C}_2 = \hat{C}_2 - C_2 \tag{16}$$

Considering the sliding mode control for which the parameters are unknown, we assume the same sliding plane given by Eq. (7). Keeping the sliding plane the same for all cases allows for direct comparison of controller performance.

The Lyapunov function is defined as follows:

$$V = \frac{1}{2}S^2 + \frac{1}{2\gamma_r}\tilde{I}_r^2 + \frac{1}{2\gamma_1}\tilde{C}_1^2 + \frac{1}{2\gamma_2}\tilde{C}_2^2 \tag{17}$$

where γ_r, γ_1, and γ_2 are positive constants. Taking the first derivative of V along the trajectory gives

$$V' = SS' + \frac{\tilde{I}_r\tilde{I}_r'}{\gamma_r} + \frac{\tilde{C}_1\tilde{C}_1'}{\gamma_1} + \frac{\tilde{C}_2\tilde{C}_2'}{\gamma_2} \tag{18}$$

Let

$$\hat{I}_r f_0(x) + \hat{C}_1 f_1(x) + \hat{C}_2 f_2(x) + p_2\alpha'' + p_1\alpha' + \hat{C}_1 g_1(x)\bar{a}_1' + \hat{C}_2 g_2(x)\bar{a}_2' = -\eta\,\mathrm{sat}(S) - kS \tag{19}$$

$$\frac{\tilde{I}_r\hat{I}_r'}{\gamma_r} + \frac{\tilde{C}_1\hat{C}_1'}{\gamma_1} + \frac{\tilde{C}_2\hat{C}_2'}{\gamma_2} - S[\tilde{I}_r f_0(x) + \tilde{C}_1 f_1(x) + \tilde{C}_2 f_2(x) + \tilde{C}_1 g_1(x)\bar{a}_1' + \tilde{C}_2 g_2(x)\bar{a}_2'] = 0 \tag{20}$$

Substituting Eqs. (19) and (20) into Eq. (18) will make V' negative-definite: $V' = -\eta|S| - kS^2 \le 0$. The update laws for the system parameters are obtained by solving Eq. (20) and they are as shown next:

$$\hat{I}_r' = \gamma_r S f_0(x), \qquad \hat{C}_1' = \gamma_1 S\psi_1, \qquad \hat{C}_2' = \gamma_2 S\psi_2 \tag{21}$$

Rearranging the terms in Eq. (19), the adaptive control laws are as follows:

$$\bar{a}_1' = \frac{\hat{D}_1}{D_1^2 + D_2^2}\hat{D}_3, \qquad \bar{a}_2' = \frac{\hat{D}_2}{\hat{D}_1^2 + \hat{D}_2^2}\hat{D}_3 \tag{22}$$

where $\hat{D}_1$, $\hat{D}_2$, and $\hat{D}_3$ take the form

$$\begin{aligned} \hat{D}_1 &= \hat{C}_1 g_1(x), \\ \hat{D}_2 &= \hat{C}_2 g_2(x), \\ \hat{D}_3 &= -\eta\,\mathrm{sat}(S) - kS - \hat{I}_r f_0(x) - \hat{C}_1 f_1(x) - \hat{C}_2 f_2(x) \\ &\quad - p_2\alpha'' - p_1\alpha' \end{aligned} \tag{23}$$

The update laws in Eq. (21) provide an estimate of the unknown parameters $\hat{I}_r$, $\hat{C}_1$, and $\hat{C}_2$ which are provided to the adaptive control laws given in Eq. (22).

2. Fault-Tolerant Adaptive Control (Case II)

For the TSS considered in this study, both tethers are made of the same material and therefore the assumption that $C = C_1 = C_2$ is valid. Hence, instead of estimating $\hat{I}_r$, $\hat{C}_1$, and $\hat{C}_2$ separately, we follow a modified system parameter representation for developing a new adaptive control law for the TSS. Taking $C = C_1 = C_2$, the expression of α''' given in Eq. (6) can be restated as

$$\eta_2\alpha''' = \eta_1 f_0(x) + [f_1(x) + f_2(x) + g_1(x)\bar{a}_1' + g_2(x)\bar{a}_2'] \tag{24}$$

where $\eta_1 = I_r/C$ and $\eta_2 = 1/C$. Therefore, the new system parameter estimates are

$$\tilde{\eta}_1 = \hat{\eta}_1 - \eta_1, \qquad \tilde{\eta}_2 = \hat{\eta}_2 - \eta_2 \tag{25}$$

To examine the convergence property of α, consider a Lyapunov function defined as follows:

$$V = \tfrac{1}{2}|\eta_2|S^2 + \tfrac{1}{2}\gamma_1\tilde{\eta}_1^2 + \tfrac{1}{2}\gamma_2\tilde{\eta}_2^2 \tag{26}$$

where γ_1 and γ_2 are positive constants. Of course, in this study, $\eta_2 = 1/C$ is always positive. Taking the derivative of V, adding and subtracting $\hat{\eta}_1 f_0(x)$ and $\hat{\eta}_2(p_2\alpha'' + p_1\alpha)$, and collecting terms gives

$$\begin{aligned} V' = {} & S[\hat{\eta}_1 f_0(x) + g_1(x)\bar{a}_1' + g_2(x)\bar{a}_2' + f_1(x) + f_2(x) \\ & + \hat{\eta}_2(p_2\alpha'' + p_1\alpha')] - \tilde{\eta}_1 S f_0(x) - \tilde{\eta}_2 S(p_2\alpha'' + p_1\alpha') \\ & + \gamma_1\tilde{\eta}_1\hat{\eta}_1' + \gamma_2\tilde{\eta}_2\hat{\eta}_2' \end{aligned} \tag{27}$$

To make $V' \le 0$, we choose the adaptation laws for canceling unknown terms as

$$\hat{\eta}_1' = \gamma_1^{-1} S f_0(x), \qquad \hat{\eta}_2' = \gamma_2^{-1} S(p_2\alpha'' + p_1\alpha') \tag{28}$$

The control inputs are obtained by solving the preceding expression for $\bar{a}_1'$ and $\bar{a}_2'$, and the adaptive control laws that guarantee asymptotic stability for the system are given by

$$\bar{a}_1' = \frac{g_1(x)}{g_1^2(x) + g_2^2(x)} g_0(x), \qquad \bar{a}_2' = \frac{g_2(x)}{g_1^2(x) + g_2^2(x)} g_0(x) \tag{29}$$

where the adaptive system parameters are specified in the term $g_0(x)$, expressed as

$$g_0(x) = \eta\,\mathrm{sat}(S) + kS + \hat{\eta}_1 f_0(x) + \hat{\eta}_2(p_2\alpha'' + p_1\alpha') \tag{30}$$

For the existence of the control laws in Eq. (33), $g_1^2(x) + g_2^2(x)$ must be nonzero in the region of interest $\Omega_S(\Omega_{S_1} \cap \Omega_{S_2})$ as formulated in Eq. (15).

C. Tether Failure

In this study, we only consider the failure of tether 2, represented by L_2 in the geometry of the TSS described in Fig. 1. The tether breakage is implemented by setting $C_2 = 0$ in the system equations of motion. Therefore,

$$\begin{aligned} & \alpha'' - 1.5 I_r \sin(2\alpha) - \frac{\lambda_1}{l_1} l[\bar{a}_1 \cos(\alpha - \beta) - \bar{b}_1 \sin(\alpha - \beta)] = 0 \\ & \beta'' + 1.5 \sin(2\beta) + 2(1 + \beta')\left(\frac{l'}{l}\right) + \frac{\lambda_1}{l_1}(1/l)[\bar{a}_1 \cos(\alpha - \beta) \\ & \quad + \bar{b}_1 \sin(\alpha - \beta)] = 0 \\ & l'' + [(1 - 3\cos^2\beta) - (1 + \beta')^2]l + \frac{\lambda_1}{l_1}[l - \bar{a}_1 \sin(\alpha - \beta) \\ & \quad - \bar{b}_1 \cos(\alpha - \beta)] = 0 \end{aligned} \tag{31}$$

The effects of this failure on the control strategies considered in this study are as follows:

1) For the case of nominal sliding mode control, if tether 2 fails, it is assumed that the failure is detected and the information is passed to the control system. Hence, the control law given by Eq. (13) simplifies to

$$\bar{a}_1' = \frac{D_3}{D_1}, \qquad \bar{a}_2' = 0 \tag{32}$$

2) For the adaptive fault-tolerant control laws considered in case I and case II, the tether failure ($C_2 = 0$) is incorporated in the system model but is not provided to the control laws.

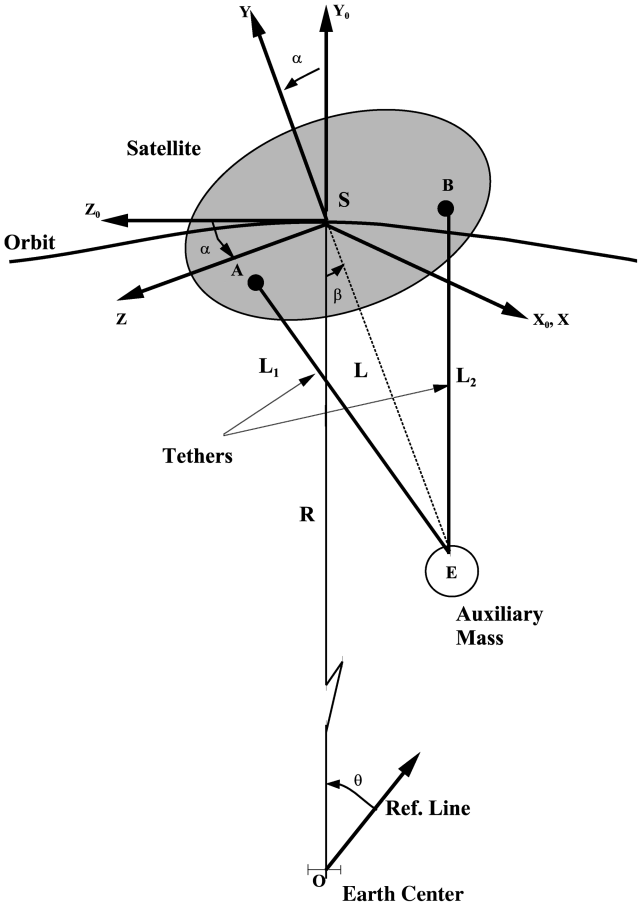

Fig. 1 Geometry of the proposed tethered satellite system.

IV. Results and Discussion

To study the effectiveness and performance of the proposed attitude control strategies, the detailed system response is numerically simulated using the set of governing equations of motion (2–5) in conjunction with the proposed control laws (13), (22), and (29). The integration is carried out using the International Mathematical and Statistical Library (IMSL) routine DDASPG based on the Petzoid–Gear backward differentiation formula method [40]. The equilibrium and desired states of the system are $\alpha_e = \alpha_d = 0$, $\alpha_e' = \alpha_d' = 0$, and $\alpha_e'' = \alpha_d'' = 0$. For simulation of the attitude response, the system parameters are chosen in dimensionless form. This enhances the scope for application of these results, regardless of the satellite size. The equations were nondimensionalized with respect to the subsatellite mass m_2, the tether reference length l_{ref}, and the orbital rate Ω. The nondimensional system parameters and initial conditions considered in this study are indicated in Table 1.

Unless otherwise stated, all the cases considered in this study are subjected to initial conditions specified in Table 1. Figure 2 shows the uncontrolled response of the TSS with tether breakage undergoing initial disturbances specified in Table 1. In the absence of a controller, the TSS is expected to exhibit the behavior seen in Fig. 2.

Table 1 Simulation parameters

Parameter	Values
Mass ratio, I_r	1
Unstretched tether lengths, l_{j0}	$l_{10} = l_{20} = 10$
Tether rigidity parameter, C_j	$C_1 = C_2 = 2 \times 10^7$
Initial offset	
Local horizontal, $\bar{a}_{j0}$	$\bar{a}_{10} = \bar{a}_{20} = 0.2$
Local vertical, $\bar{b}_{j0}$	$\bar{b}_{10} = \bar{b}_{20} = 0.5$
Initial conditions $\{\alpha, \alpha', \beta, \beta'\}$	$\{0, 0.1, 0, 0.01\}$
Occurrence of tether breakage	at 0.1 orbit

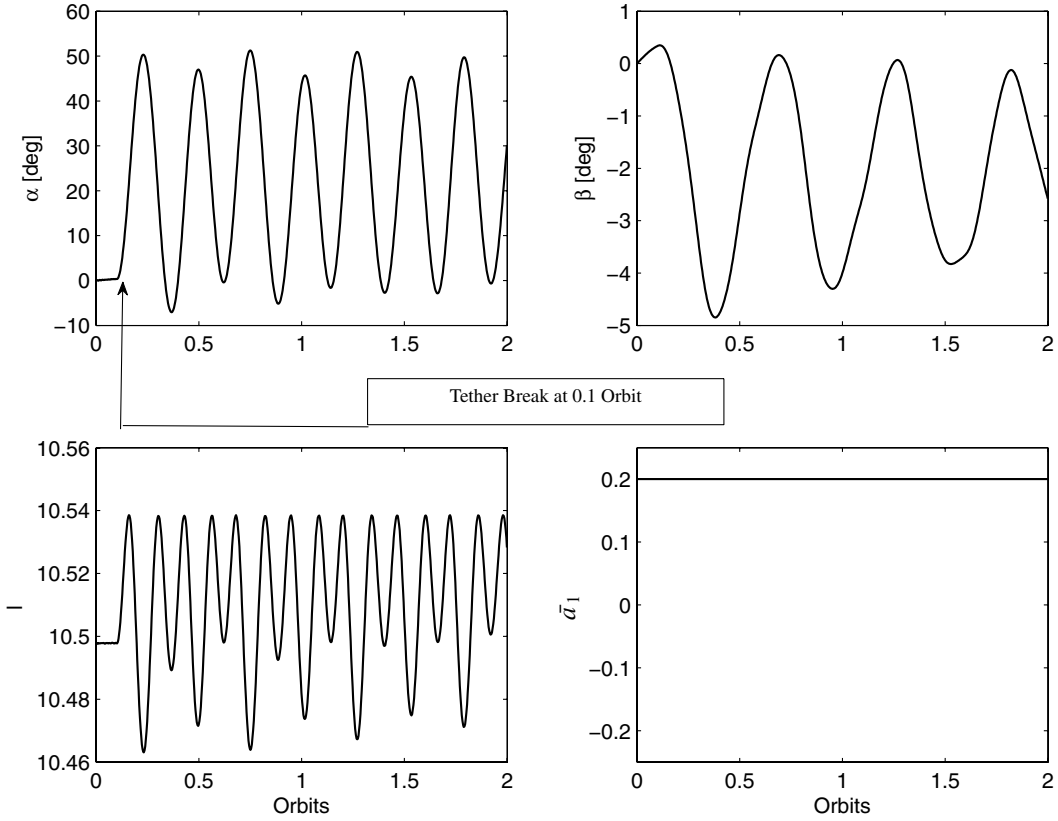

Fig. 2 Uncontrolled response of TSS when subjected to initial disturbances and tether failure at 0.1 orbit.

Although the trajectories stay bounded, they experience sustained and repeated oscillations. The objective is to bring the pitch motion of the spacecraft back to its equilibrium position ($\alpha_e = 0$). Because the response of the system under no control input is known, we can now investigate the performance of the proposed control strategies.

A. Nominal Sliding Mode Control

Figure 3 shows the controlled response of the system using the nominal sliding mode offset control scheme. The controller was numerically simulated using the following sliding mode parameter values:

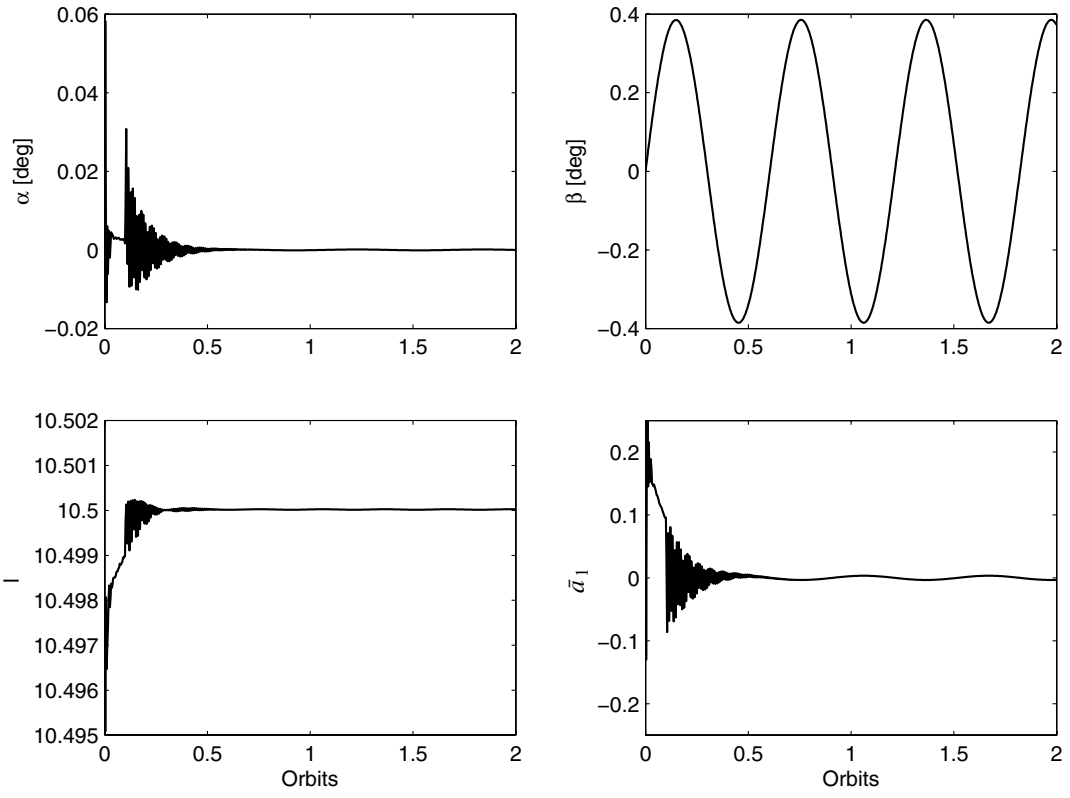

Fig. 3 Controlled response of TSS using nominal sliding mode control during tether break at 0.1 orbit.

$$p_1 = 300n, \qquad p_2 = 0.4n, \qquad \eta = 0.4, \qquad k = 10 \tag{33}$$

The values of n are fine-tuned to get a good response of the satellite pitch angle. For $n = 47,000$, it is clearly evident from Fig. 3 that the sliding mode controller is able to stabilize the attitude motion of the satellite. It is also interesting to note that even for high gains used in the sliding surfaces, the tether offset variations remain within ± 0.2 initially and gradually settle down to a value of zero. The offset regulator does not return the system to the equilibrium state corresponding to the terminal position of the attachment point ($\bar{a}_{10} = 0.2$). Because of the severance of one of the tethers, the equilibrium position of the system will pertain to $\bar{a}_1 = 0$, because the offset corresponding to the other tether does not exist. The nominal sliding mode control has proven to be very effective in stabilizing the pitch motion of the satellite.

We next examine the effect of adding external disturbances to the system between specified orbit ranges. The disturbance model is described by

$$\alpha'' = g(\alpha, \alpha', \beta, \beta', l, l', \bar{a}_1, \bar{a}_2) + d_1 \tag{34}$$

where $d_1 = 0.4$ is a lump disturbance that includes the parameter variations and other external disturbances. This disturbance is nondimensional and is activated for a specified time frame: 0.7 to 1.3 orbits. For a TSS constituting a microsatellite (60 kg, $I_x = 18.2\ \text{kg} \cdot \text{m}^2$) and an auxiliary mass (10 kg) in a 500-km circular orbit, this disturbance torque will be approximately equal to $2 \times 10^{-4}\ \text{N} \cdot \text{m}$. Figure 4 shows the effect of external disturbances on the system response. The addition of external disturbance is expected to cause certain variations in the response of the system, and the performance of sliding mode controller is investigated for this scenario. It is clearly evident from Fig. 4 that the proposed control strategy is able to overcome the external disturbances and progressively reduce the attitude errors.

The advantage of using a nonlinear controller under such circumstances can only be observed if the control responses are compared with the performance of a linear controller. The proposed linear controller to vary the tether offset is a proportional–derivative controller:

$$\bar{a}_1 = -(\mu_1 \alpha' + \nu\alpha), \qquad \bar{a}_2 = (\mu_1 \alpha' + \nu\alpha) \tag{35}$$

The linear control gains are chosen as $\mu_1 = 0.001$ and $\nu = 20$. The nonlinear control law developed in Eq. (13) was linearized and compared with Eq. (35), and then the gains were selected based on p_1 and p_2 in Eq. (33). Rather than adopting a trial-and-error procedure, the aforementioned method is more systematic for comparison of both the control laws. The controlled response of using a linear controller for the TSS undergoing initial in-plane attitude disturbances and external disturbances when the system is subjected to tether failure at 0.1 orbit is shown in Fig. 5. It is clearly evident that the proposed sliding mode controller has an advantage over the linear controller when external disturbances are added to the system. The linear controller is ineffective in damping the pitch response of the main satellite (α).

B. Fault-Tolerant Adaptive Control

We next investigate the effect of varying system parameters on the performance the system. For case I, an adaptive control law proposed in Eq. (22) is used for simulating the attitude response. The controller was numerically simulated using the following sliding plane parameter values:

$$p_1 = 300n, \qquad p_2 = 0.4n, \qquad \eta = 0.4, \qquad k = 5 \tag{36}$$

The value of $n = 420$ was chosen for the adaptive controller, compared with the large value chosen for the nominal sliding mode controller. The initial parameter estimates are taken as follows:

$$\hat{I}_{r_0} = 0.5, \qquad \hat{C}_{1_0} = 2 \times 10^5, \qquad \hat{C}_{2_0} = 2 \times 10^5 \tag{37}$$

The parameters in the plant are considered to be the same as mentioned in Table 1. Figure 6 presents the response of the system using the adaptive fault-tolerant control law in Eq. (22). When compared with the controller response obtained using the sliding mode controller in Fig. 3, it is clearly evident that the adaptive controller performs better in damping the oscillations of the pitch attitude. The overshoot and frequency of oscillations in the pitch motion is also found to be reduced considerably when compared with

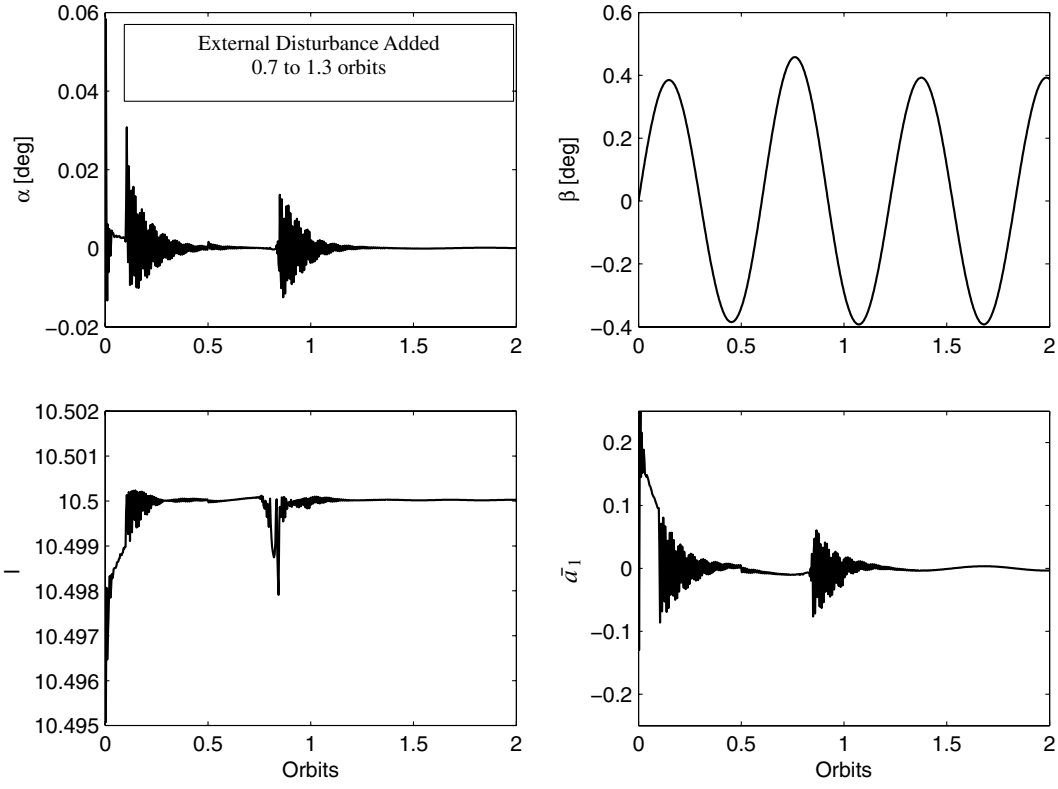

Fig. 4 Controlled response of TSS using nominal sliding mode when subjected to external disturbances.

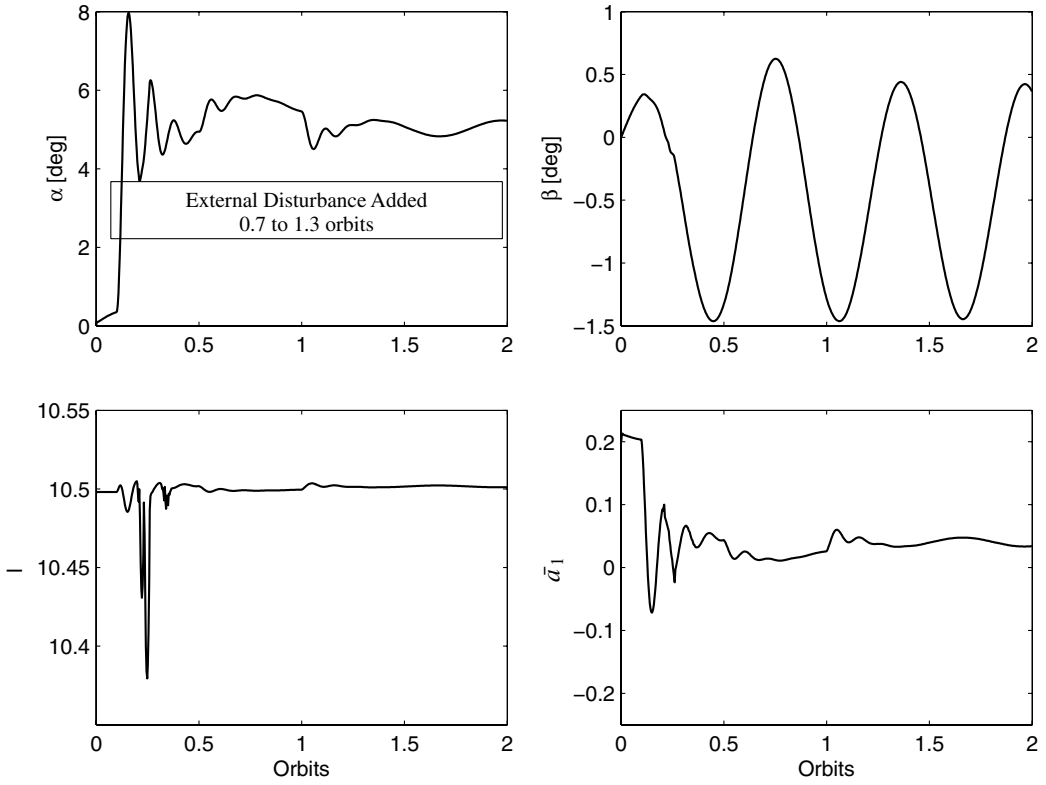

Fig. 5 Controlled response of TSS using a linear controller subjected to external disturbances.

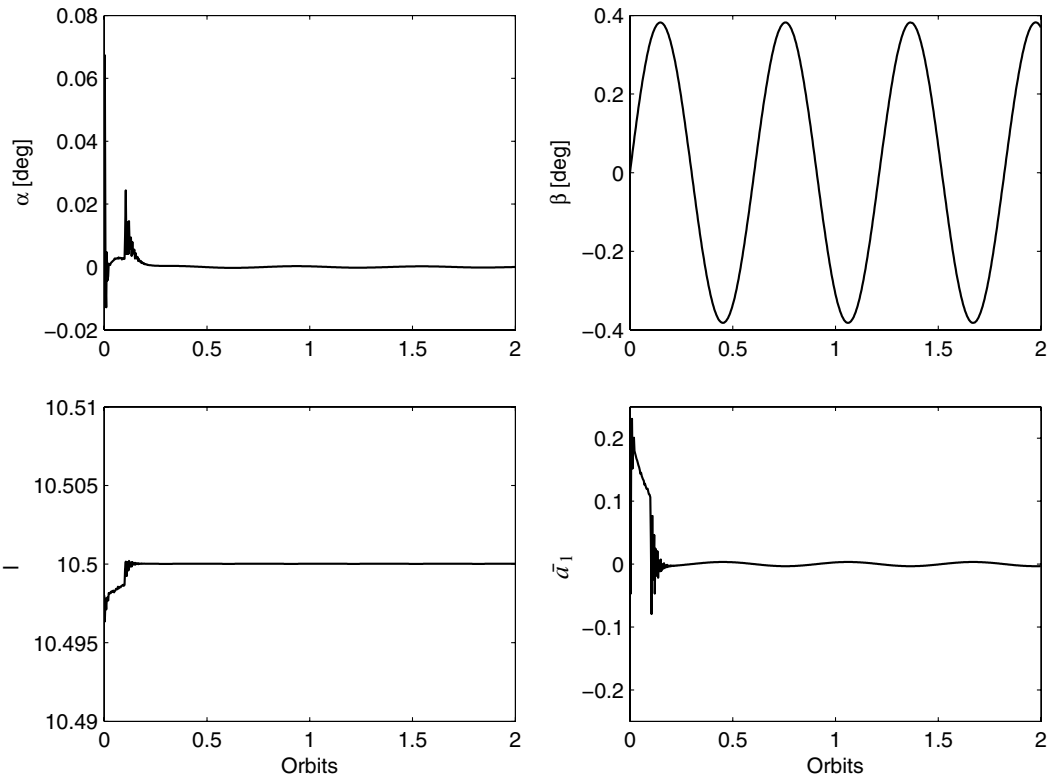

Fig. 6 Controlled response of TSS during tether break at 0.1 orbit using the adaptive control law in case I.

Fig. 3. Another important point to note here is the use of lesser gains when compared with the nominal sliding mode controller. The plot of parameter estimates are shown in Fig. 7. The constants for the adaptation laws were chosen as

$$\gamma_r = 1.8, \qquad \gamma_1 = \gamma_2 = 1.2 \tag{38}$$

At the point at which the second tether fails, the estimate of the satellite mass distribution parameter $\hat{I}_r$ reaches a value close to 3 and then settles to a value of 1. The value of $\hat{C}_i$ does not vary much, but a much lower value is used for the controller than that used in the system. Therefore, the control laws stabilize the pitch motion of the TSS and adapt very well to varying system parameters.

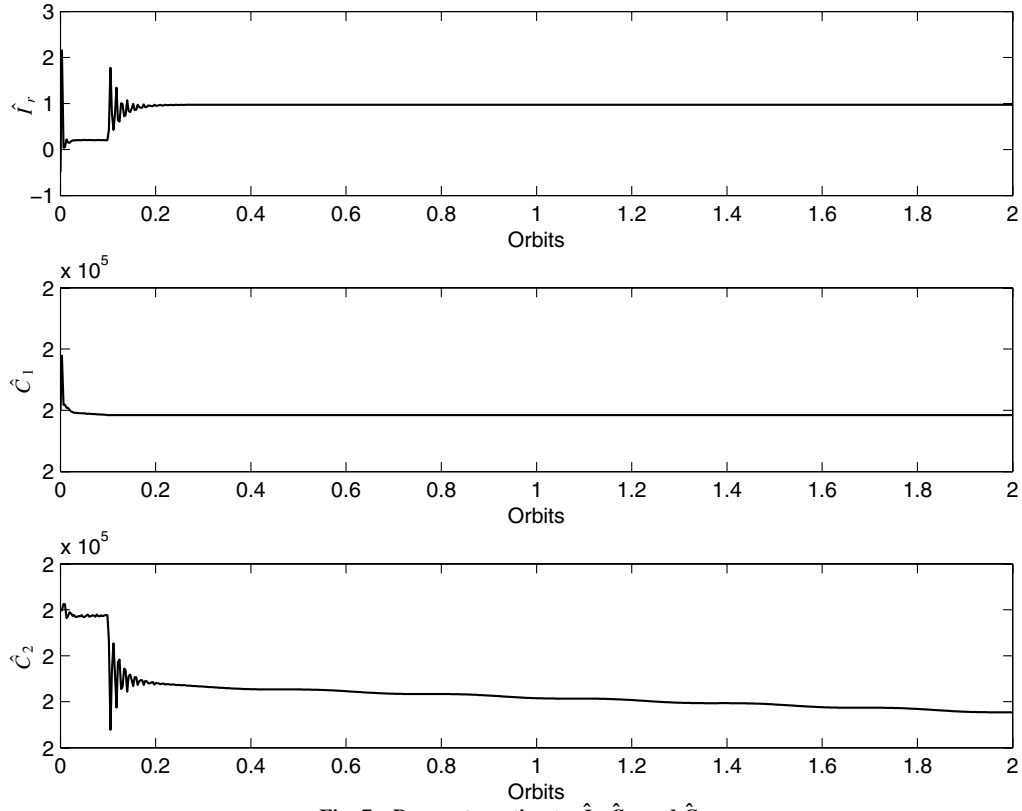

Fig. 7 Parameter estimates $\hat{I}_r$, $\hat{C}_1$, and $\hat{C}_2$.

For case II, an adaptive control law described by Eq. (33) is simulated and the results are presented next. The following sliding plane constants and adaptive gains were used:

$$p_1 = 4, \quad p_2 = 4, \quad \eta = 0.01, \quad k = 2, \quad \gamma_1 = 0.0012, \quad \gamma_2 = 0.08 \tag{39}$$

The initial parameter estimates are assumed to be

$$\hat{\eta}_1|_{\text{initial}} = \frac{I_{r0}}{C_0} = \frac{0.5}{2 \times 10^5}, \qquad \hat{\eta}_2|_{\text{initial}} = \frac{1}{C_0} = \frac{1}{2 \times 10^5} \tag{40}$$

The controlled response of the system after undergoing initial in-plane disturbances and breakage of tether 2 is shown in Fig. 8. It is

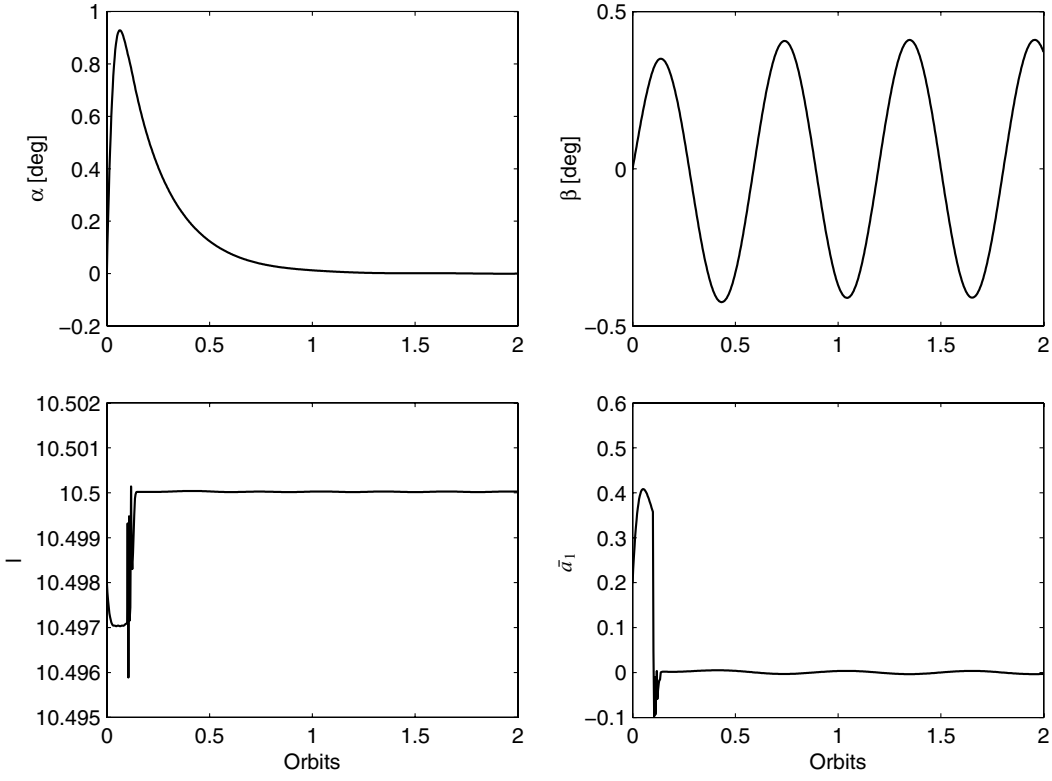

Fig. 8 Controlled response of TSS using adaptive controller in case II during tether failure at 0.1 orbit.

evident that the trajectory of α is very smooth, unlike the responses obtained from using sliding mode control (Fig. 3) and case I adaptive control (Fig. 6). One can clearly see from Fig. 8 that the system requires more settling time, compared with Figs. 3 and 6. The tradeoff is the use of much lower gains, compared with the sliding mode control and adaptive control developed in case I. This is clearly visible by comparing Eqs. (33) and (36) to Eq. (39). The control input $\bar{a}_1$ clearly counteracts for the failure of tether 2 and hence reduces its effect on the response of α. Slight distortions in the response of α occur, although it is not very clear in Fig. 8. The variation of system parameters represented by $\hat{\eta}_1 = \hat{I}_r/\hat{C}$ and $\hat{\eta}_2 = 1/\hat{C}$ is shown in Fig. 9. These values, although extremely high compared with the ideal case (Table 1), prove the robustness of this adaptive control scheme.

1. Random Initial Conditions

We next examine the results from a wider range of system parameters and initial disturbances to make the conclusions more generally applicable. The adaptive fault-tolerant control scheme developed in Sec. III.B.2 is tested for random system parameters. The saturation limit for the controller is set at $\bar{a}_1 = \pm 0.4$. For the random simulations, the control gains were chosen as

$$p_1 = 6, \qquad p_2 = 6, \qquad \eta = 0.1, \qquad \phi = 0.3, \qquad K = 3 \tag{41}$$

Figure 10 shows the range of system parameters that gave successful results for two sets of initial disturbances: 1) $\alpha'_0 = 0.1$ and $\beta'_0 = 0.01$ and 2) $\alpha'_0 = 0.1$ and $\beta'_0 = 0.01$. Tether breakage at 0.1 orbit was simulated. It can be clearly observed from Fig. 9 that for the case of $\alpha'_0 = 0.1$ and $\beta'_0 = 0.01$, a wider range of system parameters were successful in controlling the response of the system during the failure of one of the tethers. The initial unstretched length of the tether, l_{j_0}, had no effect on the analysis. Therefore, for any initial tether length, the range of $\bar{a}_j$ and $\bar{b}_j$ remains the same. As the disturbance was increased to $\alpha'_0 = 0.1$ and $\beta'_0 = 0.01$, the maximum initial horizontal offset available was $\bar{a}_j = 0.27$ for $\bar{b}_j = 0.6$. Keeping initial disturbances the same, we then examined the effect of control gains on a range of system parameters. Figure 11 shows the range of system parameters that were successful in controlling the response of the system for two cases: 1) $K = 3$ and 2) $K = 5$. Using $K = 5$, for $\bar{b}_j = 0.6$, the maximum available initial offset is increased to 0.32 as opposed to the case of $\bar{a}_j = 0.27$ for $K = 3$. Therefore, the range of system parameters for which the fault-tolerant adaptive control provides successful results depend on the gains and the initial disturbances considered. For larger disturbances, the range of system parameters decreases. Tuning the control gains can also help in increasing the range of system parameters.

2. Tether Attachment-Point Blocking

Grassi et al. [41] studied a control system that integrates a reaction wheel and a mobile attachment point onboard each of two tethered platforms. They considered a breakdown case in which the attachment-point control system on the mother satellite stops work and only the daughter satellite attachment point provides the two-satellite pitch and roll control. Because the controller developed in Sec. III.B case II is termed as fault-tolerant, we next incorporate the more likely fault scenario in which one of the offset jams in position. An abrupt stop of the tether attachment point $\bar{a}_2$ at 0.1 orbit is simulated and the results are shown in Fig. 12. No modifications were made to the control law in Eq. (29), to accommodate for offset blockage. It can be clearly observed that $\bar{a}_1$ overshoots to a value of 0.4 as soon as $\bar{a}_2$ is jammed at 0.17; $\bar{a}_1$ eventually settles at 0.17 after controlling the pitch attitude of the main satellite. As expected, even when one of the offsets is stuck in position, the fault-tolerant controller proposed in this study demonstrates excellent performance in providing pitch control.

3. Tether Attachment-Point Sign Reversal

We consider the case in which one of the tether attachment points starts moving with sign reversal. Although the control laws provide the correct signal, a fault in the actuator can reverse the motion of the tether attachment point. Figure 13 shows the librational motion of the main satellite for a case in which $\bar{a}_2$ starts moving with sign reversal after 0.1 orbit. The fault-tolerant adaptive control methodology [Eq. (29)] proposed in this study can effectively damp the oscillations present in the pitch attitude even when one of the offsets start moving with sign reversal.

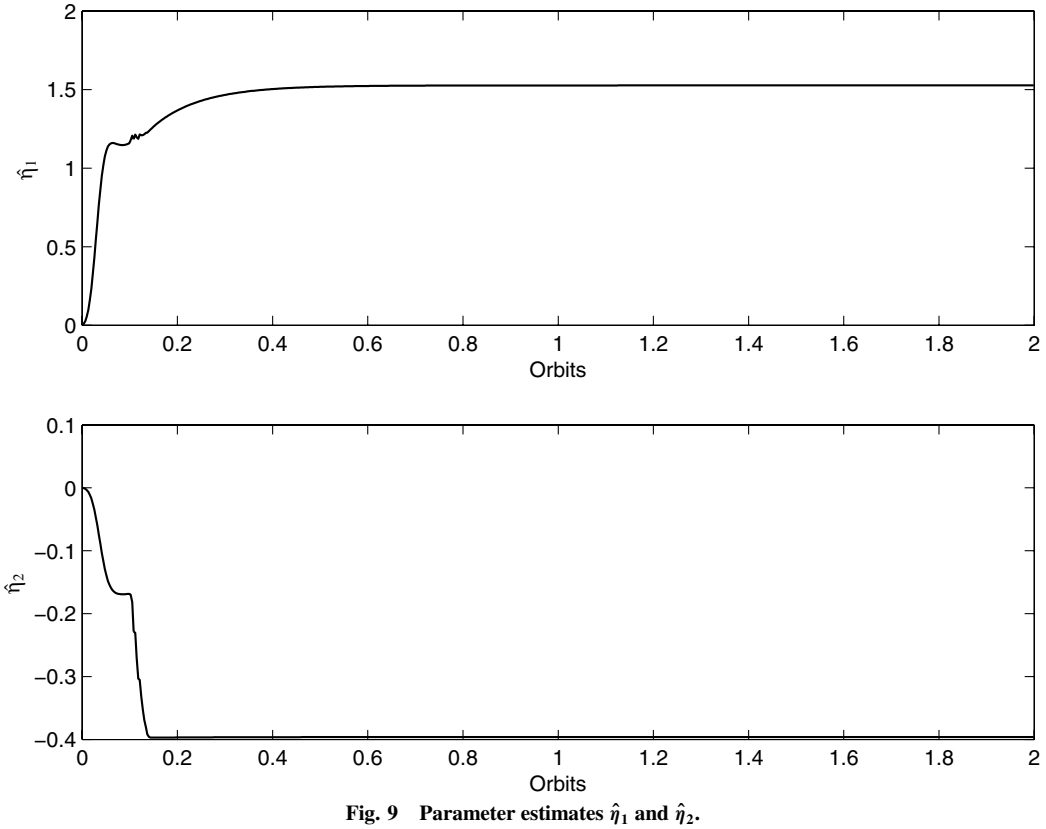

Fig. 9 Parameter estimates $\hat{\eta}_1$ and $\hat{\eta}_2$.

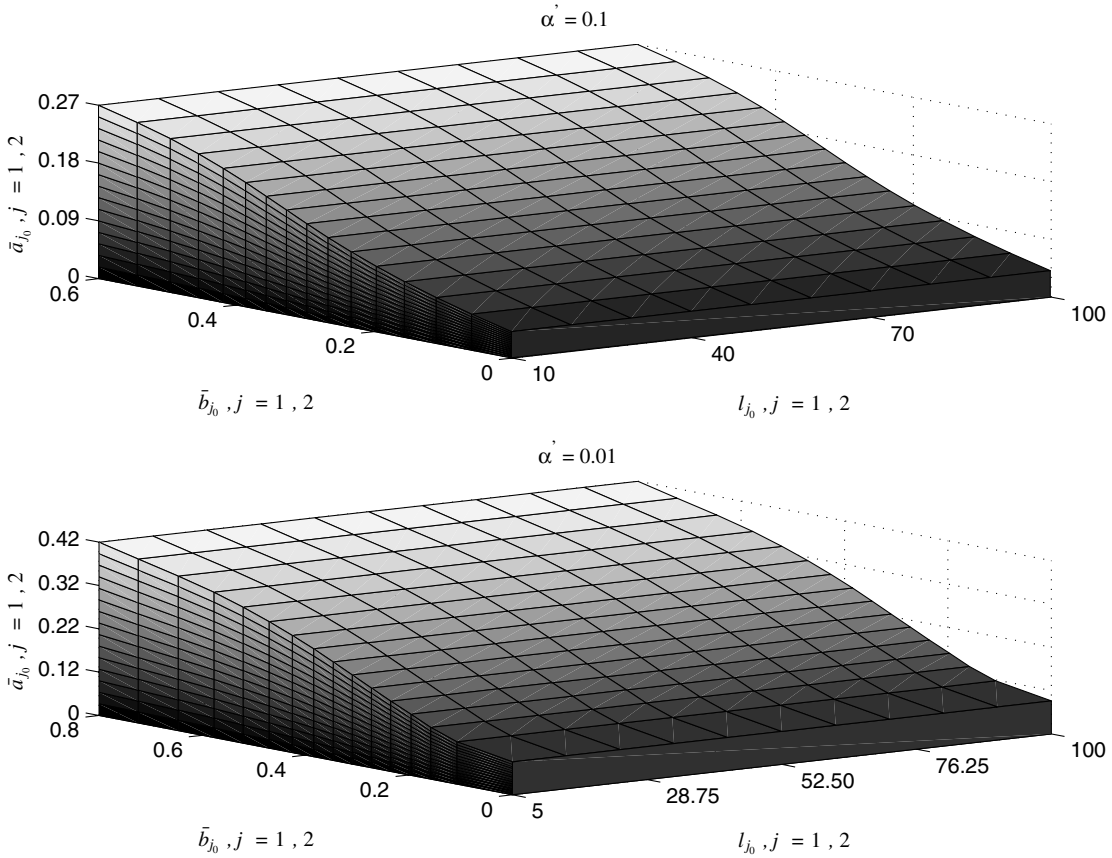

Fig. 10 Range of system parameters giving stable solution for $\alpha' = 0.1$ and 0.01.

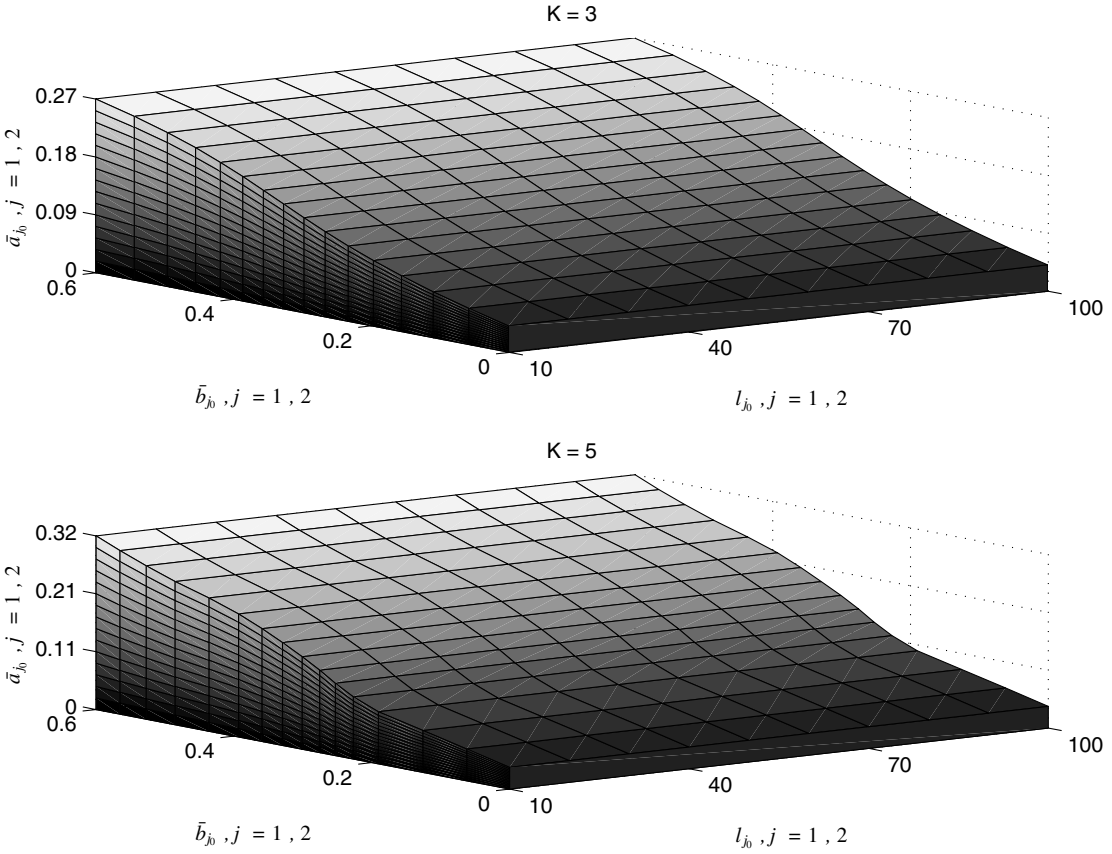

Fig. 11 Range of system parameters giving stable solution for control gains $K = 3$ and 5.

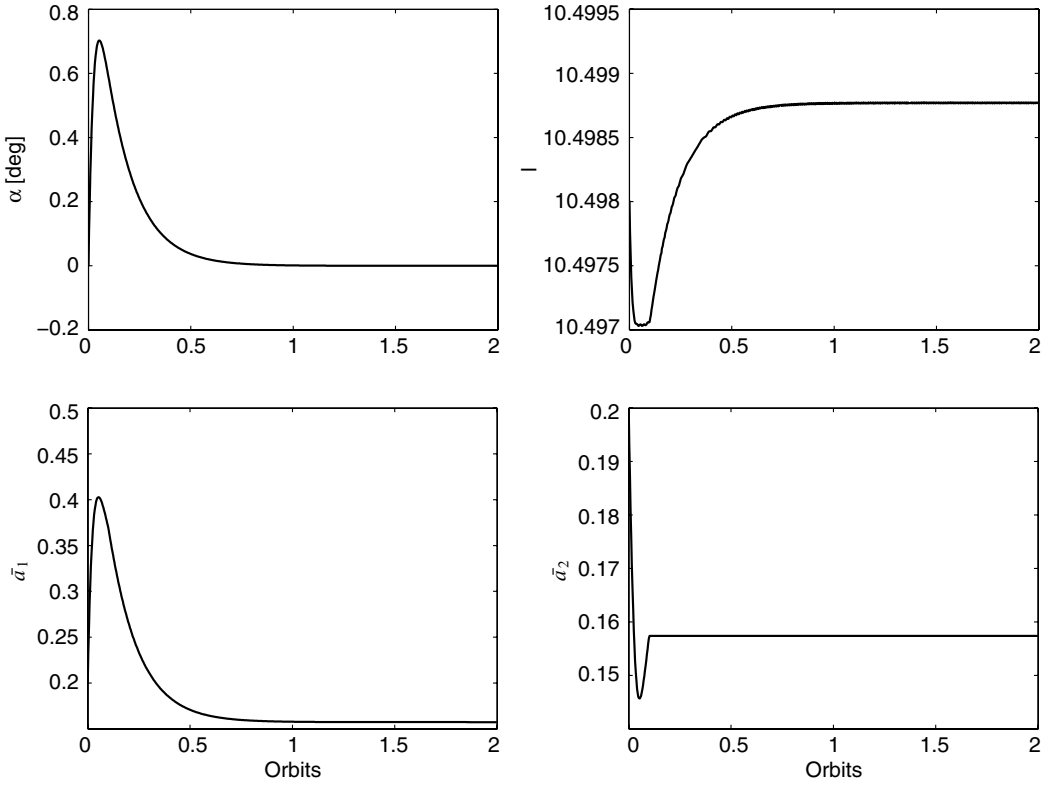

Fig. 12 Controlled response of TSS when the breakdown of the $\bar{a}_2$ attachment point is simulated at 0.1 orbit.

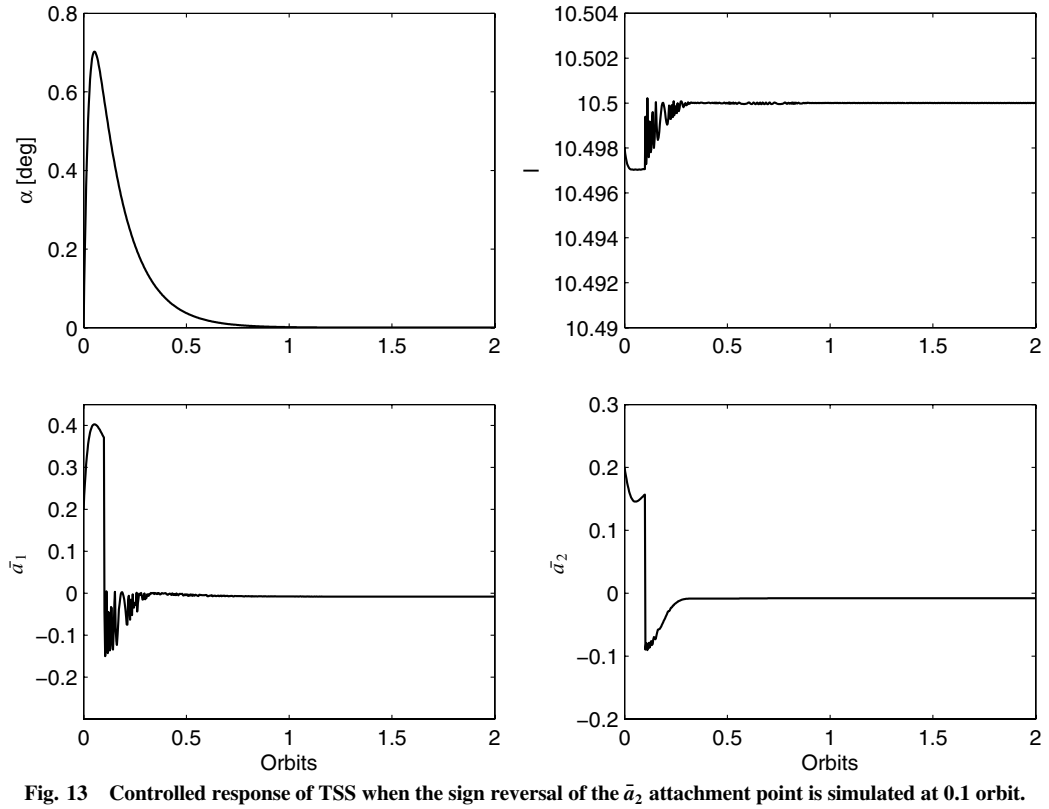

Fig. 13 Controlled response of TSS when the sign reversal of the $\bar{a}_2$ attachment point is simulated at 0.1 orbit.

C. Quantitative Analysis

Based on the results obtained in this section, it is important to examine whether the maximum tether offset variations required for the fault-tolerant adaptive controllers can satisfy the requirements of real satellites. Depending on the size of the satellite, the actual tether offset will be a_1 in dimension. The maximum tether offset a_1 required for attitude maneuver of TSS of various sizes is presented in Table 1.

For SPARTNIK, a diameter of 0.51 m gives a maximum of 0.2 m for a_1 and a_2. The requirement from the simulation in dimensionless form is $\bar{a}_1 = 0.4$, which can be converted to $a_1 = 0.1$ m in dimensions using the satellite parameters in Table 2. This clearly falls

Table 2 Maximum tether offset requirements for various satellite systems

Satellites	Mass, kg	Auxiliary mass, kg	Size, m	Moment of inertia, kg · m^2	Maximum tether offset, m	Maximum offset speed, m/s
Microsatellite SPARTNIK	40	5	Diameter = 0.51 Height = 0.25	$I_x = 0.324$ $I_y = 0.303$ $I_z = 0.486$	0.1	0.3
Nanosatellite MUSTANG0	8.335	1	Diameter = 0.4 Height = 0.3	$I_x = 0.137$ $I_y = 0.178$ $I_z = 0.176$	0.14	0.2
Picosatellite YAMSAT	1	0.09	Length = 0.1 Depth = 0.1 Height = 0.1	$I_x = 0.001$ $I_y = 0.002$ $I_z = 0.001$	0.4	0.7

under the maximum available value of 0.2 m. Similarly for nanosatellites and picosatellites, the maximum tether offset requirements are met very comfortably. The maximum speed requirements for the offsets vary from 0.3 m/s for a microsatellite to 0.7 m/s for a picosatellite (Table 2). For the practical realization of the proposed control strategy, several issues, including power and weight requirements, must be taken into account.

The preceding results bring out powerful features of the proposed adaptive controllers (cases I and II). The performance of the controller does not deteriorate even when the system parameters are changing and yet provides a better attitude response, as seen in Figs. 6 and 8. It is seen that in the closed-loop dynamics, the estimated parameters do not converge to their true values in Figs. 7 and 9. Furthermore, the proposed controllers perform satisfactorily even in the case of a slack tether. Overall, tether offset variations using sliding mode control prove to be an excellent control strategy for TSS even when one of the tether fails.

One of the major advantages of employing a two-tether satellite system over a single-tether system is the level of redundancy introduced into the system if one of the tethers were to be severed. However, as discussed in Sec. I, there are some ill effects that must be taken into account when a tether breaks. There is a huge possibility that the remaining tether could collide with itself and lead to tether entanglement. These cases were not considered in the simulations. This paper primarily deals with the design of an adaptive fault-tolerant control law that can stabilize the attitude motion of the main spacecraft even if one of the tethers were to be severed.

V. Conclusions

The paper presents the fault-tolerant adaptive stabilization of a TSS using and offset control scheme in the presence of tether failure. The numerical integration of the governing nonlinear equations of motion establishes the feasibility of the proposed tether offset variation strategy. The equations of motion were developed using the Lagrangian approach. Based on a nominal sliding mode technique, two different types of nonlinear adaptive controllers were designed. The controllers also include parameter adaptation laws. A nonadaptive controller based on sliding mode technique was also developed for comparing a linear proportional–derivative control law when external disturbance is added to the system. Based on the numerical simulations, the following main conclusions can be drawn:

1) The proposed nominal sliding mode control law for changing tether offsets is very effective in stabilizing the attitude of the satellite about its nominal equilibrium position when subjected to initial attitude disturbances and occurrence of tether breakage.

2) The effect of additional external disturbances on the system for a particular period in the orbit was studied. Even in the most demanding situations, the controller is able to overcome the disturbances and stabilize the attitude of the spacecraft. The results were compared with a linear controller for which the performance deteriorated under the presence of external disturbances.

3) The adaptive sliding mode controller developed in case I damped the pitch motion of the main satellite with low control gains when compared with the nominal sliding mode controller. The controller is able to withstand variation in system parameters.

4) The adaptive sliding mode controller developed using modified representation of system parameters (case II) outperforms the other control strategies developed in this study. Use of low sliding mode gains and better adaptation to tether failure are the advantages of this approach. The adaptive controller was also tested for cases when one of the tether attachment point abruptly stops moving and when one of the offsets moves with sign reversal. This control strategy demonstrated excellent performance in all the fault and failure cases considered.

The proposed control methodologies are able to stabilize the satellite's attitude within a quarter of an orbit using tether offsets to the order of one-tenth of a meter for small satellites. Overall, the numerical results clearly establish the robustness of the proposed adaptive offset control scheme in regulating the satellite dynamics of a two-tether system in the event of breakage of one of the tethers.

Appendix

I. Derivation of Equations of Motion

The generalized variables related through dimensionless constraints are as follows:

$$\begin{aligned} f_1 &= l_1 - (\bar{a}_1^2 + \bar{b}_1^2 + l^2 - 2l\bar{h}_1)^{\frac{1}{2}} = 0, \\ f_2 &= l_2 - (\bar{a}_2^2 + \bar{b}_2^2 + l^2 + 2l\bar{h}_2)^{\frac{1}{2}} = 0 \end{aligned} \tag{A1}$$

where

$$\begin{aligned} \bar{h}_1 &= \bar{a}_1 \sin(\alpha - \beta) + \bar{b}_1 \cos(\alpha - \beta), \\ \bar{h}_2 &= \bar{a}_2 \sin(\alpha - \beta) - \bar{b}_2 \cos(\alpha - \beta), \\ l_j &= l_{j0}(1 + \varepsilon_j) \quad (j = 1, 2) \end{aligned} \tag{A2}$$

To apply the Lagrangian approach for the formulation of the system equations of motion, the expressions for the system kinetic energy (T) as well as the potential energy (V) are first obtained:

$$T = \tfrac{1}{2}M(\dot{R}^2 + \dot{\theta}^2 R^2) + \tfrac{1}{2}m_2[\dot{L}^2 + (\dot{\theta} + \dot{\beta})^2 L^2] + \tfrac{1}{2}I_x(\dot{\theta} + \dot{\alpha})^2 \tag{A3}$$

$$\begin{aligned} V = &-\frac{\mu M}{R} + \frac{1}{4}\frac{\mu}{R^3}[(I_x + I_y + I_z) - 3\{I_x + (I_z - I_y)\cos 2\alpha\}] \\ &+ \frac{1}{2}\frac{\mu}{R^3} m_2[1 - 3\cos^2\beta]L^2 + \frac{1}{2}EA\sum_{j=1}^{2} L_{jo}\varepsilon_j^2 u_j \end{aligned} \tag{A4}$$

The term u_j [also denoted later as $U(\varepsilon_j)$] in the potential energy expression is simply a unit function, the use of which precludes any negative strain in the tether:

$$U(\varepsilon_j)|_{j=1,2} = \begin{cases} 1, & \text{for } \varepsilon_j \geq 0 \\ 0, & \text{for } \varepsilon_j < 0 \end{cases} \tag{A5}$$

The Lagrangian equations of motion corresponding to the various generalized coordinates indicated earlier may be obtained using the general relation

$$\frac{\mathrm{d}}{\mathrm{d}t}\left[\frac{\partial T}{\partial \dot{q}}\right]-\frac{\partial T}{\partial q}+\frac{\partial V}{\partial q}=Q+\sum_{j=1}^{2}\Lambda_j\frac{\partial f_j}{\partial q} \tag{A6}$$

where q denotes the vector of generalized coordinates, Q denotes the generalized force corresponding to the generalized coordinate q, and Λ_j denotes the Lagrange multiplier corresponding to the jth constraint. Substituting the generalized coordinates in Eq. (A6) and carrying out the algebraic manipulation, we obtain the governing nonlinear coupled ordinary differential equations of motion. The equation of tether strains [Eq. (5)] was derived from the following relations.

Tether strain ε_1:

$$EA_1L_{10}\varepsilon_1U(\varepsilon_1)=\Lambda_1 l_{10} \tag{A7}$$

Tether strain ε_2:

$$EA_2L_{20}\varepsilon_2U(\varepsilon_2)=\Lambda_2 l_{20} \tag{A8}$$

The tether strains given in Eqs. (A7) and (A8) can be nondimensionalized by using the following expression:

$$\lambda_j=\frac{\Lambda_j}{m_2L_{\mathrm{ref}}^2\Omega^2},\qquad j=1,2 \tag{A9}$$

Substituting Eq. (A9) into Eqs. (A7) and (A8) gives

Tether strain ε_1:

$$\lambda_1=C_1\varepsilon_1U(\varepsilon_1) \tag{A10}$$

Tether strain ε_2:

$$\lambda_2=C_2\varepsilon_2U(\varepsilon_2) \tag{A11}$$

II. Derivation of α'''

To substitute for the α''' term, we first consider the spacecraft pitch equation of motion in Eq. (2), which can be also written in the following form:

$$\alpha''=1.5I_r\sin(2\alpha)+C_1E_1A_1l-C_2E_2A_2l \tag{A12}$$

where E_j and A_j take the form given by

$$\begin{aligned}
&E_j=\left[\frac{1}{l_{j0}}-\frac{1}{l_j}\right],\qquad \frac{\lambda_j}{l_j}=C_jE_j\quad (j=1,2),\\
&\bar{A}_1=\bar{a}_1\cos(\alpha-\beta)-\bar{b}_1\sin(\alpha-\beta),\\
&\bar{A}_2=\bar{a}_2\cos(\alpha-\beta)+\bar{b}_2\sin(\alpha-\beta)
\end{aligned} \tag{A13}$$

Taking the third derivative of α from Eq. (A12), the detail of the dynamics of the system is explored so that a first-order derivative of the control input can be explicitly obtained:

$$\begin{aligned}
\alpha'''=&I_rf_0(x)+C_1E_1\bar{A}_1l'+C_1E_1\bar{A}_1'l+C_1E_1'\bar{A}_1l\\
&-C_2E_2\bar{A}_2l'-C_2E_2\bar{A}_2'l-C_2E_2'\bar{A}_2l
\end{aligned} \tag{A14}$$

The new derivative terms in Eq. (A14) can be rearranged to extract $\bar{a}_1'$ and $\bar{a}_2'$ using the following expressions:

$$\begin{aligned}
&f_0(x)=3\cos(2\alpha)\alpha'\\
&\bar{A}_1'=\bar{a}_1'\cos(\alpha-\beta)-\bar{a}_1\sin(\alpha-\beta)(\alpha'-\beta')\\
&\quad-\bar{b}_1\cos(\alpha-\beta)(\alpha'-\beta')=\bar{a}_1'\cos(\alpha-\beta)+\bar{A}_{11}'\\
&\bar{A}_2'=\bar{a}_2'\cos(\alpha-\beta)-\bar{a}_2\sin(\alpha-\beta)(\alpha'-\beta')\\
&\quad+\bar{b}_2\cos(\alpha-\beta)(\alpha'-\beta')=\bar{a}_2'\cos(\alpha-\beta)+\bar{A}_{22}'
\end{aligned} \tag{A15}$$

From Eq. (A1), it is evident that $\bar{a}_1'$ and $\bar{a}_2'$ will also appear when l_1 and l_2 are differentiated. The first derivatives of $\bar{h}_1$ and $\bar{h}_2$ [defined in Eq. (A2)] are given by

$$\begin{aligned}
&E_1'=\frac{l_1'}{l_1^2}\qquad E_2'=\frac{l_2'}{l_2^2}\\
&\bar{h}_1'=\bar{a}_1'\sin(\alpha-\beta)+\bar{a}_1\cos(\alpha-\beta)(\alpha'-\beta')\\
&\quad-\bar{b}_1\sin(\alpha-\beta)(\alpha'-\beta')=\bar{a}_1'\sin(\alpha-\beta)+\bar{h}_{11}'\\
&\bar{h}_2'=\bar{a}_2'\sin(\alpha-\beta)+\bar{a}_2\cos(\alpha-\beta)(\alpha'-\beta')\\
&\quad+\bar{b}_2\sin(\alpha-\beta)(\alpha'-\beta')=\bar{a}_2'\sin(\alpha-\beta)+\bar{h}_{22}'
\end{aligned} \tag{A16}$$

Using the preceding relations, l_1' and l_2' are given by

$$\begin{aligned}
l_1'&=\frac{1}{l_1}[\bar{a}_1\bar{a}_1'+ll'-\bar{h}_1l'-(\bar{a}_1'\sin(\alpha-\beta)+\bar{h}_{11}')l]\\
&=\left[\frac{\bar{a}_1-l\sin(\alpha-\beta)}{l_1}\right]\bar{a}_1'+l_{11}'\\
l_2'&=\frac{1}{l_2}[\bar{a}_2\bar{a}_2'+ll'+\bar{h}_1l'+(\bar{a}_1'\sin(\alpha-\beta)+\bar{h}_{11}')l]\\
&=\left[\frac{\bar{a}_2+l\sin(\alpha-\beta)}{l_2}\right]\bar{a}_2'+l_{22}'
\end{aligned} \tag{A17}$$

The new form of α''' after substituting Eqs. (A15–A17) into Eq. (A14) is given by

$$\begin{aligned}
\alpha'''=&I_rf_0(x)+C_1E_1\bar{A}_1l'+C_1E_1[\bar{a}_1'\cos(\alpha-\beta)+\bar{A}_{11}']l\\
&+C_1\left(\left[\frac{\bar{a}_1-l\sin(\alpha-\beta)}{l_1^3}\right]\bar{a}_1'+\frac{l_{11}'}{l_1^2}\right)\bar{A}_1l\\
&-C_2E_2\bar{A}_2l'-C_2E_2[\bar{a}_2'\cos(\alpha-\beta)+\bar{A}_{22}']l\\
&-C_2\left(\left[\frac{\bar{a}_2+l\sin(\alpha-\beta)}{l_2^3}\right]\bar{a}_2'+\frac{l_{22}'}{l_2^3}\right)\bar{A}_2l
\end{aligned} \tag{A18}$$

The parameters I_r, C_1, and C_2 are also considered for modeling parametric uncertainties for adaptive control. Therefore, making further simplifications to Eq. (A18), we obtain

$$\begin{aligned}
&f_0(x)=3\cos(2\alpha)\alpha',\quad f_1(x)=E_1A_1l'+E_1\bar{A}_{11}'l+\bar{A}_1\frac{l_{11}'}{l_1^2}l,\\
&f_2(x)=-E_2A_2l'-E_2\bar{A}_{22}'l-\bar{A}_2\frac{l_{22}'}{l_2^2}l\\
&g_1(x)=\bar{A}_1\left[\frac{\bar{a}_1-l\sin(\alpha-\beta)}{l_1^3}\right]l+E_1\cos(\alpha-\beta)l\\
&g_2(x)=-\bar{A}_2\left[\frac{\bar{a}_2+l\sin(\alpha-\beta)}{l_2^3}\right]l-E_2\cos(\alpha-\beta)l
\end{aligned} \tag{A19}$$

The new form of α''', along with $\bar{a}_1'$ and $\bar{a}_2'$ appearing explicitly, is shown in Eq. (A20):

$$\alpha'''=I_rf_0(x)+C_1f_1(x)+C_2f_2(x)+C_1g_1(x)\bar{a}_1'+C_2g_2(x)\bar{a}_2' \tag{A20}$$

References

[1] Colombo, G., Goposchkin, E. M., Grossi, M. D., and Weiffenback, G. C., "Shuttle-Borne Skyhook: A New Tool for Low-Orbital-Altitude Research," Smithsonian Inst. Astrophysical Observatory CR NAS8-02138, Cambridge, MA, Sept. 1974.

[2] Cosmo, M. L., and Lorenzini, E. C., (eds.), *Tethers in Space Handbook*, 3rd ed., NASA, Washington, D.C., 1997.

[3] Tyc, G., and Han, R. P. S., "Attitude Dynamics Investigation of the OEDIPUS-A Tethered Rocket Payload," *Journal of Spacecraft and Rockets*, Vol. 32, No. 1, 1995, pp. 133–141. doi:10.2514/3.26585

[4] Tyc, G., Vigneron, F. R., Jablonski, A. M., Han, R. P. S., Modi, V. J., and Misra, A. K., "Flight Dynamics Results from the OEDIPUS-C Tether Mission," AIAA Paper 96-3573, July 1996.

[5] Smith, H. F., "The First and Second Flights of the Small Expandable Deployer System (SEDS)," *Proceedings of the Fourth International Conference on Tethers in Space*, Vol. 1, Science and Technology Corp., Hampton, VA, 1995, pp. 43–55.
[6] Jost, R. J., and Chlouber, D., "Plasma Motor Generator Mission Report," *Proceedings of the 4th International Conference on Tethers in Space*, Vol. 1, Science and Technology Corp., Hampton, VA, 1995, pp. 149–163.
[7] Purdy, W., Coffery, S., Barnds, W. J., Kelm, B., and Davis, M., "TiPS —Results of a Tethered Satellite Experiment," *Advances in the Astronautical Sciences*, Vol. 97, Pt. 1, Aug. 1997, pp. 3–23.
[8] Tomlin, D. D., Mowery, D. K., Musetti, B., and Cibrario, B., "TSS Mission 1 Flight Dynamics Anomalies," *Proceedings of the Fourth International Conference on Tethers in Space*, Vol. 1, Science and Technology Corp., Hampton, VA, 1995, pp. 119–132.
[9] Zedd, M. F., "Experiments in Tether Dynamics Planned for ATEX's Flight," *Advances in the Astronautical Sciences*, Vol. 97, Pt. 1, Aug. 1997, pp. 25–44.
[10] Kumar, K. D., "Review of Dynamics and Control of Non-electrodynamic Tethered Satellite Systems," *Journal of Spacecraft and Rockets*, Vol. 43, No. 4, 2006, pp. 705–720. doi:10.2514/1.5479
[11] Misra, A. K., and Modi, V. J., "Dynamics and Control of Tether Connected Two-Body Systems—A Brief Review," *Space 2000*, edited by L. G. Napolitano, AIAA, Washington, D.C., 1983, pp. 473–514.
[12] Misra, A. K., and Modi, V. J., "A Survey on the Dynamics and Control of Tethered Satellite Systems," *Advances in the Astronautical Sciences*, Vol. 62, Sept. 1986, pp. 667–719.
[13] Misra, A. K., and Diamond, G. S., "Dynamics of a Subsatellite System Supported by Two Tethers," *Journal of Guidance, Control, and Dynamics*, Vol. 9, No. 1, 1986, pp. 12–16.
[14] Kumar, K., and Kumar, K. D., "Line-of-Sight Pointing Stability for Drifting Satellites," *IEEE Transactions on Aerospace and Electronic Systems*, Vol. 35. No. 2, Apr. 1999, pp. 504–510. doi:10.1109/7.766932
[15] Modi, V. J., "Spacecraft Attitude Dynamics: Evolution and Current Challenges," *Acta Astronautica*, Vol. 21, No. 10, 1990, pp. 689–718. doi:10.1016/0094-5765(90)90097-5
[16] Bainum, P. M., Woodard, S., and Juang, J. N., "The Development of Optimal Control Laws for Orbiting Tethered Platform Systems," *Advances in the Astronautical Sciences*, Vol. 58, Pt. 1, Aug. 1985, pp. 219–314.
[17] Fan, R., and Bainum, P. M., "Dynamics and Control of a Space Platform with a Tethered Subsatellite," *Journal of Guidance, Control, and Dynamics*, Vol. 11, No. 4, 1988, pp. 377–381. doi:10.2514/3.20324
[18] Lemke, L. G., Powell, J. D., and He, X., "Attitude Control of Tethered Spacecraft," *Journal of the Astronautical Sciences*, Vol. 35, No. 1, 1987, pp. 41–55.
[19] Kline-Schoder, R. J., and Powel, J. D., "Precision Attitude Control for Tethered Satellites," *Journal of Guidance, Control, and Dynamics*, Vol. 16, No. 1, 1993, pp. 168–174.
[20] Kumar, K. D., and Nakajima, A., "Angular Momentum Damping of Debris Through Tether System," *Proceedings of the 22nd International Symposium on Space Technology and Science*, edited by Y. Arakawa, 2000, pp. 1780–1785.
[21] Modi, V. J., Lakshmanan, P. K., and Misra, A. K., "Offset Control of Tethered Satellite Systems: Analysis and Experimental Verification," *Acta Astronautica*, Vol. 21, No. 5, 1990, pp. 283–294. doi:10.1016/0094-5765(90)90089-4
[22] Modi, V. J., Lakshmanan, P. K., and Misra, A. K., "Offset Control Strategy for the Space Station Based Tethered Payload," *Journal of the Astronautical Sciences*, Vol. 39, No. 2, 1991, pp. 205–232.
[23] Modi, V. J., Lakshmanan, P. K., and Misra, A. K., "On the Control of Tethered Satellite Systems," *Acta Astronautica*, Vol. 26, No. 6, 1992, pp. 411–423. doi:10.1016/0094-5765(92)90070-Y
[24] Pradhan, S., Modi, V. J., and Misra, A. K., "Tethered Platform Coupled Control," *Acta Astronautica*, Vol. 44, No. 5, 1999, pp. 243–256. doi:10.1016/S0094-5765(99)00014-4
[25] Modi, V. J., Pradhan, S., and Misra, A. K., "Offset Control of Tethered Satellite Systems Using a Graph Theoretic Approach," *Acta Astronautica*, Vol. 35, No. 6, 1995, pp. 373–384. doi:10.1016/0094-5765(94)00286-U
[26] Grassi, M., and Cosmo, M. L., "Attitude Dynamics of the Small Expendable-Tether Deployment System," *Acta Astronautica*, Vol. 36, No. 3, 1995, pp. 141–148. doi:10.1016/0094-5765(95)00093-F
[27] Grassi, M., and Cosmo, M. L., "Atmospheric Research with the Small Expendable Deployer System: Preliminary Analysis," *Journal of Spacecraft and Rockets*, Vol. 33, No. 1, 1996, pp. 70–78. doi:10.2514/3.55709
[28] Modi, V. J., Gilardi, G., and Misra, A. K., "Attitude Control of Space Platform Based Tethered Satellite System," *Journal of Aerospace Engineering*, Vol. 11, No. 2, 1998, pp. 24–31. doi:10.1061/(ASCE)0893-1321(1998)11:2(24)
[29] Kumar, K. D., and Kumar, K., "Attitude Maneuver of Dual Tethered Satellite Platforms through Tether Offset Change," *Journal of Spacecraft and Rockets*, Vol. 38, No. 2, 2001, pp. 237–242.
[30] Pines, D. J., Flotow, A. H., and Redding, D. C., "Two Nonlinear Control Approaches for Retrieval of a Thrusting Tethered Subsatellite," *Journal of Guidance, Control, and Dynamics*, Vol. 13, No. 4, 1990, pp. 651–658.
[31] Walls, J., and Greene, M., "Adaptive Control of an Orbiting Single Tether System," *Proceedings of the Twenty-First Southeastern Symposium on Systems Theory*, Inst. of Electrical and Electronics Engineers, Piscataway, NJ, Mar. 1989, pp. 594–598.
[32] Nohmi, M., Nenchev, D. N., and Uchiyama, M., "Tethered Robot Casting Using a Spacecraft-Mounted Manipulator," *Journal of Guidance, Control, and Dynamics*, Vol. 24, No. 4, 2001, pp. 827–833.
[33] Williams, P., Watanabe, T., Blanksby C., Trivailo, P., and Fuiji, H. A., "Libration Control of Flexible Tethers Using Electromagnetic Forces and Movable Attachment," *Journal of Guidance, Control, and Dynamics*, Vol. 27, No. 5, 2004, pp. 882–897. doi:10.2514/1.1895
[34] Trivailo, P., Fujii, H. A., and Blanksby C., "Safety Implications of Unscheduled Situations in the Operation of Tethered Satellite Systems from International Space Station," *Acta Astronautica*, Vol. 44, No. 7, 1999, pp. 701–707. doi:10.1016/S0094-5765(99)00060-0
[35] Williams, P., Blanksby C., Trivailo, P., Fuiji, H. A., and Kojima, H., "Dynamics and Control of Platform-Supported Two-Tether Subsatellite System," *Advances in the Astronautical Sciences*, Vol. 117, Dec. 2003, pp. 245–264.
[36] Blanksby C., and Trivailo, P., "Collision Dynamics of Space Tethers," *Journal of Guidance, Control, and Dynamics*, Vol. 23, No. 6, 2000, pp. 1078–1081.
[37] Slotine, J. J. E., and Li, W., *Applied Nonlinear Control*, Prentice–Hall, Upper Saddle River, NJ, 1991, pp. 122–126.
[38] Fernandez, B. R., and Hedrick, J. K., "Control of Multivariable Non-Linear Systems by the Sliding Mode Method," *International Journal of Control*, Vol. 46, No. 3, 1987, pp. 1019–1040. doi:10.1080/00207178708547410
[39] Slotine, J. J. E., and Sastry, S. S., "Sliding Controller Design for Non-Linear Systems," *International Journal of Control*, Vol. 40, No. 2, 1984, pp. 421–434. doi:10.1080/00207178408933284
[40] International Mathematical and Statistical Library (IMSL), Math Library, Ver. 3.0, Visual Numerics, Inc., Houston, TX, 1997.
[41] Grassi, M., Moccia, A., and Vetrella, S., "Tethered System Attitude Control After Attachment Point Blocking," *Acta Astronautica*, Vol. 32, No. 5, 1994, pp. 355–362. doi:10.1016/0094-5765(94)90157-0

D. Spencer
Associate Editor